Published in final edited form as:
Exp Eye Res. 2008 June ; 86(6): 914–928. doi:10.1016/j.exer.2008.03.008.

Postreceptoral contributions to the light-adapted ERG of mice lacking b-waves

Suguru Shirato, **Hidetaka Maeda**, **Gen Miura**, and **Laura J. Frishman****
University of Houston College of Optometry, 4901 Calhoun Rd, 505 JDA, Houston, TX, 77204-2020

Abstract

The purpose of this study was to determine the contributions of postreceptoral neurons to the light-adapted ERG of the *Nob* mouse, a model for complete-type congenital stationary night blindness (CSNB1) that lacks a b-wave from depolarizing bipolar cells. Ganzfeld ERGs were recorded from anesthetized adult control mice, control mice injected intravitreally with L-2-amino-4-phosphonobutyric acid (Control APB mice) to remove On pathway activity, and *Nob* mice. ERGs also were recorded after PDA (*cis*-2, 3-piperidine-dicarboxylic acid, 3–5 mM) was injected to block transmission to hyperpolarizing (Off) bipolar and horizontal cells, and all 3rd order neurons. Stimuli were brief (< 4 ms, 0.4 – 2.5 log sc td s) and long (200 ms, 2.5 – 4.6 log sc td) LED flashes (λmax = 513 nm, on a rod suppressing background (2.6 log sc td). Sinusoidal modulation of the LEDs (mean, 2.6 log sc td; contrast, 100%; 3 to 36 Hz) was used to study flicker ERGs.

Brief-flash ERGs of *Nob* mice presented as long-lasting negative waves with a positive-going intrusion that started about 50 ms after the flash and peaked around 120 ms. Control APB mice had similar responses, and in both cases, PDA removed the positive-going intrusion. For long flashes, PDA removed a small, slow “d-wave” after light offset. With sinusoidal stimulation, the fundamental (F1) amplitude of control mice ERG peaked at 8 Hz (~70 μV). For *Nob* mice the peak was ~20 μV at 6 Hz before PDA and ~10 μV at 3 Hz or lower after PDA. F1 responses were present up to 21 Hz in control and *Nob* eyes and 15 Hz in *Nob* eyes after PDA. Between 3 and 6 Hz, F1 phase was 170°–210° more delayed in *Nob* than control mice; phase was hardly altered by PDA. With vector analysis, a substantial postreceptoral input to the *Nob* flicker ERG was revealed. In control mice, the second harmonic (F2) response showed peaks of ~10 μV at 3 Hz and 13 Hz. *Nob* mice showed almost no F2. In summary, in this study it was found that in *Nob* mice, postreceptoral neurons from the Off pathway make a positive-going contribution to the light-adapted flash ERG, and contribute substantially to sinusoidal flicker ERG.

Keywords

Retina; Electroretinogram; Light-adapted ERG; Flicker ERG; b-wave; *Nob* mouse; Congenital stationary night blindness

**Correspondence to: Laura J. Frishman, University of Houston, College of Optometry, 4901 Calhoun Rd, 505 J. Davis Armistead Bldg., Houston, TX 77204-2020, Phone: 713-743-1972, Fax: 713-743-2595, E-mail: lfrishman@uh.edu.

Financial disclosures: There are no financial disclosures

Conflict of Interest: There are no conflicts to report.

INTRODUCTION

Absorption of quanta by vertebrate photoreceptors causes them to hyperpolarize which reduces the amount of glutamate that they release. This change in transmitter release is detected by two major categories of bipolar cells in the retina, depolarizing (DBCs) and hyperpolarizing bipolar cells (HBCs). The HBCs are contacted mainly but not exclusively by cone rather than rod photoreceptors (Tsukamoto et al., 2001), and have ionotropic glutamate receptors on their dendrites that lead to sign conserving, hyperpolarizing responses to light onset, and depolarizing responses to light offset. In contrast, the DBCs in both rod and cone pathways have G-protein-coupled metabotropic glutamate receptors (mGluR6) that lead, via a biochemical cascade, to sign inverting responses such that onset of a light stimulus causes the cells to depolarize and offset, to hyperpolarize. These two different cone bipolar cell types are the initial neurons of parallel On and Off pathways that traverse the retina and are maintained in central pathways to the primary visual cortex.

Defects in signal transmission between photoreceptors and bipolar cells result in various functional abnormalities that are detectable in the electroretinogram (ERG). Congenital stationary night blindness (CSNB) is a family of retinal disorders characterized by night blindness from birth. Patients with complete, X-linked CSNB (CSNB-1) have an essentially total loss of the ERG b-wave under light, and dark-adapted conditions, and a profound loss of rod-mediated vision (e.g. Miyake et al., 1986 e.g. Miyake et al., 1887; Pesch et al., 2000). Blockade of transmission between photoreceptors and DBCs by a glutamate analogue the binds to mGlur6 receptors, APB (L-2-amino-4-phosphonobutyric acid), similarly results in no ERG b-wave under photopic and scotopic conditions in the macaque retina, a retina very similar to that of humans (Khan et al., 2005; Knapp & Schiller, 1984; Sieving et al., 1994), and in the retina of normal mice (Kang Derwent et al., 2007; Sharma et al., 2005), In contrast, blockade of transmission from photoreceptors to HBCs using an iontotropic glutamate receptor antagonist in macaques and mice results in a reduced photopic ERG a-wave and in macaques, elimination of the d-wave (Maeda et al., 2003; Sharma et al., 2005; Sieving et al., 1994).

CSNB-1 is due to mutation of the *Nyx* gene localized to Xp11.4 that encodes a novel protein, nyctalopin (Bech-Hansen et al., 2000; Bergen et al., 1996; Boycott et al., 1998; Rozzo et al., 1999). The *Nob* mouse also has a mutation in nyctalopin (Gregg et al., 2003; Pesch et al., 2003). As in humans with CSNB-1, the *Nob* ERG lacks a b-wave [as indicated by the name, no b-wave (*Nob*)], although the corneal negative a-wave looks normal (Candille et al., 1999; Pardue et al., 1998). Expression of Nyx has been found to be strong in mouse retina INL, using *in situ* hybridization (Gregg et al., 2003), and transgenic rescue of the mutated nyctalopin can restore function (Demas et al., 2006; Gregg et al., 2007). The *Nob* mouse is now sometimes termed the *Nob1* mouse because other no b-wave mice, numbering up to *Nob4*, to date, with different mutations have been characterized. For example, *Nob4* (Pinto et al., 2007) is a murine model for patients with mutations in the GRM6 gene encoding mGluR6 (Dryja et al., 2005).

Although *Nob* mice have a defect in synaptic transmission between photoreceptors and depolarizing bipolar cells, retinal layer thicknesses are similar in the *Nob* mice and their unaffected littermates (Pardue et al., 1998), indicating that postreceptoral neurons are present in normal numbers in *Nob* mice. It also has been shown that the absence of nyctalopin in *Nob* mice does not disrupt the expression pattern of other proteins required for synaptic transmission (Ball et al., 2003). Given the relatively normal appearance of the retina, the postreceptoral components of the ERG originating from hyperpolarizing bipolar cells and 3rd order neurons should still be present in the response, although recent ganglion cell recordings show abnormalities in inner retinal activity beyond those expected for a defect localized to On bipolar cells (Demas et al., 2006; Gregg et al., 2007).

Electroretinograms of normal mice (and rats) do not evidence d-waves (Sharma et al., 2005; Xu et al., 2001), a typical reflection of the Off pathway contribution to the flash ERG (e.g. Sieving et al., 1994). Pharmacologic blockade studies using APB also have not revealed d-waves in rodents (Sharma et al., 2005; Xu et al., 2001). The *Nob* mouse presents an opportunity to look more closely at postreceptoral contributions to mouse ERG from the Off pathway. In this study, we investigated the role of postreceptoral neurons in generating the mouse light-adapted ERG by application of pharmacological agents in *Nob* and normal mouse retinas. Based on our findings, we can now describe a positive-going component from postreceptoral neurons in the Off pathway that was present in the *Nob* retina and in retinas of congenic control mice or normal c57BL/6 mice injected with APB. Postreceptoral components also could be seen to contribute to the flicker ERG of mice lacking b-waves. This work was summarized in an abstract (Shirato et al., 2005).

METHODS

Subjects

Subjects were adult C57BL/6NCRSim (hereafter C57BL/6) mice three to six months of age (9 mice, 14 eyes) or one year of age (2 mice, 4 eyes) (Simonsen Labs, USA); male *Nob* mice three to six months of age (3 mice, 6 eyes and 2 congenic littermates) or *Nob* mice one year of age (6 mice, 8 eyes) (all from Dr. Machelle Pardue). The *Nob* mutation was originally identified on a BALB/cByJ background and was crossed later to C57BL/6J mice (Pardue et al., 1998). Animals were screened for the *Nob* mutation as previously described (Kang Derwent et al., 2007; Pardue et al., 1998). The mice were all housed in a room with a 12 hr on (< 40 lux)/12 hr off light/dark cycle. Experimental procedures were approved by Institutional Animal Care Committee of the University of Houston, and adhered to the ARVO Statement for the Use of Animals in Ophthalmic and Vision Research.

ERG recording

Animals were initially anesthetized with ketamine (60 mg/kg) and xylazine (6 mg/kg) via an intraperitneal injection and anesthesia was maintained with ketamine (56 mg/kg) and xylazine (5.6 mg/kg) roughly every 45-minutes via a subcutaneous needle fixed in the flank as described previously for this lab (Saszik et al., 2002). The animal's head was held with a clamp that fit over the nose, and fixed the two front teeth in a bite bar that also served as the electrical ground. Pupils were fully dilated to 3 mm in diameter with topical atropine (0.5%), phenylephrine (2.5%) and tropicamide. Body temperature was maintained between 37–38° C with a thermostatically controlled electrically heated blanket (CWE, Inc., Ardmore, PA, USA). Recording sessions lasted 4 to 8 hours. Nearly all of the mice recovered from anesthesia after each session.

For most experiments ERG responses to LED stimuli were recorded differentially between DTL fiber electrodes that were moistened with methylcellulose sodium (Celluvisc, Allergan Inc, USA) and placed on the corneas under contact lenses: a clear contact lens (ACLAR film, Honeywell, USA) on the tested eye and a black contact lens (PVC) and black foil over the non-tested eye and the skull. For the paired flash experiment that used a high energy probe flash in the ColorDome of the Espion stimulator (Diagnosys LLC, USA), recordings were made differentially between DTL fiber electrodes placed under the clear contact lens on tested eye and subcutaneously in the cheek below the tested eye.

Visual stimulation

In all experiments, stimuli were presented on a rod suppressing LED background (2.6 log sc td, λ max = 513 nm) to which animals were adapted for at least 45 minutes before recording. This long adaptation time ensured full recovery of a-wave amplitude in the presence of the

background (Kaneko et al., 2006; Ueda et al., 2006). Responses were averaged over many trials. Signals were amplified 10,000X (0.1 to 300 Hz), filtered to remove 60 Hz and digitized at 1 KHz.

Flash ERG experiments—The stimuli were ganzfeld flashes of short duration (<4 ms, 0.4 – 2.5 log sc td s) and long duration (200 ms, 2.5 – 4.6 log sc td) provided by LEDs (λ max = 513 nm) in the mini-ganzfeld ColorBurst stimulator of the Espion system. Flash intervals were 1.0 second (short flash) and 1.5 second (long flash). This stimulus presented on a rod-saturating background would have elicited responses dominated by medium wavelength (M−) cones in the mouse, although some rod signal may have been present at the long adaptation times that were used (Kaneko et al., 2006). A photometer, scotopically corrected for human rods, (International Light model IL1700), was used to measure the luminance (sc cd m^{-2}) from which luminous energy (sc cd m^{-2} s^{-1}) was calculated for the brief flashes whose durations (< 4 ms) were under the integration time for the neurally generated retinal signals that we were measuring in the ERG. Because the stimulus was a green LED, contributions from UV-driven responses (with peak sensitivity around 360 nm) were minimal, and the scotopic calibration was nearly correct for the reported mouse M-cone peak sensitivity of 509–512 nm (Jacobs et al., 2004). Retinal illuminances (in sc td for backgrounds and long flashes) were calculated for a pupil diameter of 3 mm with no correction for the Stiles-Crawford effect. For the brief flashes the energy was reported in sc td s.

Flicker experiments—The stimulus was created by sinusoidal modulation of LEDs (mean illuminance 2.6 log sc td; λ max = 513 nm; contrast, 100 %; 3 to 36 Hz).

Paired flash experiments—Strimuli were paired flashes (test flash, 1.3–3.7 log sc td s; probe flash, 3.7 log sc td s) presented in the Espion ColorDome for a range paired flash intervals (5 ms – 400 ms). The intertrial interval between each paired flash set was 6 seconds.

Intravitreal injection

Under a dissecting microscope (10X) a small hole was punctured in the eye just behind the limbus with a 27-gauge needle, and a glass pipette needle (tip ~ 20 μm) was inserted through the hole as described in Kang Derwent et al., 2007 for experiments on the dark-adapted ERG of Nob mice. Pharmacological agents, L-2-amino-4-phosphonobutyric acid (APB) (1.6 – 2.0 mM) to eliminate on bipolar cell light responses (Slaughter and Miller, 1981), cis-2,3-piperidinedicarboxylic acid (PDA) (5.2 – 6.2 mM) to block Off bipolar and inner retinal light responses (Slaughter and Miller, 1983; Massey, 1990 for review), and a mixed solution of APB +PDA (same concentrations as reported for each) were injected into the eye (1.0 – 1.5 μl) using a Hamilton microsyringe. (Hamilton Company, Reno, NV). Vitreal concentrations of drugs were based on a vitreal volume of 20 μl. The ERG was monitored until no further change was seen in the response before accepting data; this delay was typically no more than an hour.

Drug injection experiments

Generally pre drug injection and post injection recordings were done in the same session, on the same eye. When two drugs were to be used, i.e. APB and APB + PDA, recordings were done before and after APB in one recording session, and before and after APB+PDA (mixed in one injection) in a later session using the fellow eye of the same mouse. Recording sessions were separated by at least a week to allow complete recovery of the animal from the time under anesthesia, and the corneas from any effects of having electrodes and contact lenses on them.

Data analysis

Single flash ERG—Standard a-wave amplitudes were measured at a fixed time (15 ms) after the brief flash. To measure the positive intrusion in *Nob* mice, and normal mice injected with APB, response amplitudes were measured at the negative peak (a-wave) and positive intrusion peak and plotted vs. stimulus energy. The amplitude of the positive intrusion was obtained by subtraction to find the difference between the negative peak amplitude and the positive intrusion peak amplitude.

Flicker ERG—The amplitudes and phases of fundamental (F1) and second (F2) harmonic Fourier components were measured from the original waveform of the flicker ERG using the FFT implemented in a MATLAB program. Fourier components of the noise were measured from a region of each record where the mean level was present but not modulated (i.e. 0 Hz) which occurred in the last 3000 ms of each 6000 ms epoch. The amplitudes of *Nob* postreceptoral components were derived using vector subtraction of *Nob* PDA results from *Nob* results.

Paired flash ERG—In order to derive the photoreceptor component of flash ERG responses, we analyzed paired flash data following a test and probe flash procedure similar to the one previously described (Kang Derwent et al., 2007; Pepperberg et al., 1997; Hetling and Pepperberg, 2001; Friedburg et al., 2004). For clarity, the method will be described in the Results section.

Statistics—For comparisons between groups, a two-sample *t*-test assuming assuming unequal variances was used. For comparison of the same eye's results before and after intravitreal injections, a paired comparison *t*-test was used.

RESULTS

Light-adapted ERG response to brief flashes

Fig. 1 shows light-adapted ERGs of Control and *Nob* mice in response to brief flashes of increasing stimulus energy. Typical control ERGs (Fig. 1A), recorded from a C57BL/6 mouse between three to six months of age, had a prominent b-wave, peaking about 45 ms after the flash, that grew in amplitude with increased flash energy. A small a-wave was present in responses to the two strongest stimuli that were used. In contrast, the response of *Nob* mice, as originally described by Pardue et al. (1998) and illustrated here in Fig. 1C, did not have a b-wave. Instead, the *Nob* response was predominantly negative-going, although a small positive intrusion could be seen in most records. The onset of the positive intrusion in the *Nob* ERG occurred soon after the b-wave in control eyes had peaked (see Fig. 1D, and the expanded ERG in Fig. 2A), and it rose slowly to a peak about 70 ms later.

Nob mice are known to have a defect in synaptic transmission between photoreceptors and On-bipolar cells. Because of this, we were interested to know whether the waveform of the ERG in control eyes would be similar to that of *Nob* mice after intravitreal injection of the glutamate analogue, APB, to eliminate transmission between photoreceptors and On-bipolar cells. Fig. 1B shows the responses of a control eye after APB. The ERGs looked similar to those of the *Nob* mouse in Fig. 1C: the post APB responses were mainly negative-going, and included a small positive intrusion. The similarity of the *Nob*, and Control APB response is better seen in Fig. 1D which shows superimposed ERGs of the Control, the Control with APB injection (Control APB) and the *Nob* mouse in response to the strongest stimulus energy, 2.5 log sc td s, in Fig. 1A–C. The larger size of the positive intrusion in the Control APB mice when the higher energy stimuli were used was a consistent finding that will be addressed in more detail later in the Results.

In this study C57BL/6 mice were used as controls because their ERGs were similar to those of the congenic littermates of the *Nob* mice, which were on a BALB/cByJ C57Bl/6J background (see methods). Fig. 1E has been included to illustrate the similarity of the responses of the congenic littermates of *Nob* mice to those of the C57BL/6 mice both before and after APB injection. The responses resemble the responses shown in Fig. 1D of Control and Control APB animals to the same stimulus.

Fig. 2A and B show the first 400 ms of the ERGs plotted using an expanded vertical axis to better illustrate the positive intrusion seen in Fig. 1. The positive intrusion in the *Nob* ERG in this figure (Fig. 2A) was typical. The intrusion started about 50 ms after the stimulus and peaked about 120 ms after. The presence of the positive intrusion thus defined the trough of the a-wave around 50 ms after the flash. The Control APB ERG had a larger positive intrusion than the intrusion in the *Nob* ERG. As shown in Fig. 2B, the intrusion in the Control APG ERG started a little earlier, creating an a-wave trough about 40 ms after the stimulus, and peaked a little sooner, about 100 ms after the flash (Fig. 2B). While Fig. 2A and B illustrate the response to the highest energy flash for single animals, the onset and peak times for the positive intrusion for *Nob* and Control mice respectively were similar for the range of stimulus energies that were used.

In order to quantify the size of the positive intrusion, responses measured at the onset and peak of the positive intrusion were plotted versus stimulus energy in the left panels of Fig. 2C for the *Nob* and 2D for the Control APB mice. The hatched areas designate the amplitude of the positive intrusion and show that it was present for all but the weakest flash energies. For each of the three highest stimulus energies the positive intrusion was larger by at least a factor of two for the Control APB mice than for the *Nob* mice, and these differences were significant ($P<0.01$, two sample *t*-test assuming unequal variances). Although the positive intrusion was larger, the a-wave amplitude measured from time of response onset to the trough was similar for the two groups, a little more than 80 μV on average for both.

Brief-flash ERGs after Intravitreal injection of PDA

As noted in the Introduction, although the *Nob* mouse ERG lacks a b-wave, it should contain postreceptoral components from the Off pathway. In order to investigate the contributions of postreceptoral neurons to the light-adapted ERG of the *Nob* mouse, we injected PDA into the vitreous humor of *Nob* mouse eyes to block the AMPA/KA receptors on Off-bipolar cells, horizontal cells, and 3rd order neurons, presumably thereby eliminating much if not all postreceptoral responses in the *Nob* retina (Slaughter and Miller, 1983; Massey, 1990 for review). Fig. 3A and B show the responses of a *Nob* mouse before and after PDA injection. After PDA, the initial fast portion of the a-wave was smaller, and the positive intrusion was no longer present. Fig. 3C and 3D show the Control APB result and Control APB+PDA result for one animal. The results look similar to those in the *Nob* mice.

The effects of PDA on the a-wave and the positive intrusion in Control APB and *Nob* mice are easier to see in the expanded plots of Fig. 2. Fig. 2A and the amplitude plot in Fig. 2C show that in *Nob* mice PDA reduced the response amplitude at the time of the negative a-wave trough to a value slightly above the peak level of the positive intrusion prior to injection. The wave then continued to become more negative, rather than more positive, in the time following 50 ms after the flash. The ERG increased in amplitude until about 80 ms after the flash, and then slowly recovered from the maximum.

In the Control APB eyes (Fig. 2A and D) the amplitude of the ERG at the time of the trough (40 ms) also was reduced after PDA injection. As in the *Nob* eye, the wave continued to become more negative in the absence of the positive intrusion up to about 80 ms after the flash, These findings indicate that the positive intrusion was generated by postreceptoral neurons in the Off

pathway in both *Nob* and Control APB eyes. A small difference between the groups after PDA injection was that negative-going response measured between 50 and 120 ms, the location of the positive intrusion for Nobs before PDA was smaller than the response measured between 40 and 100 ms for Control-APB eyes for each of the highest three stimulus energies ($P<0.005$, two sample *t*-test assuming unequal variance).

Effect of PDA on the a-wave

Average ERGs traces from three Control eyes prior to APB (solid line) in response to the strongest stimulus used in this study are shown in Fig. 4A to illustrate the timing of the a-wave maximum amplitude (trough) in normal eyes. The a-wave trough occurred between 15 and 20 ms after the flash, reaching almost −40 μV before being truncated by the b-wave. After APB injection, the leading edge of average a-wave was similar to that in the Control eyes until about 15 ms after the flash, and then in the absence of the b-wave it continued downward reaching more than −80 μV by 25 ms after the flash. The leading edge of the average *Nob* a-wave (Fig. 4B) was similar in time course to the Control APB a-wave.

After PDA injection (bold dashed lines in Fig. 4A and B) the a-waves were still similar to those before PDA for the initial 8 to 10 ms, and then they declined less steeply with time. Fig. 4C shows amplitudes measured near the time of the a-wave trough in control records (15 ms) and at the same time after PDA plotted as a function of stimulus energy. The Control, Control-APB and *Nob* responses all had almost the same a-wave amplitudes before PDA, reaching about −35 μV at the highest stimulus energy. The average a-wave amplitudes after PDA were reduced to less than −15 μV for the strongest stimulus, and were significantly different from responses before PDA for both groups for the highest two stimulus energies ($P<0.01$, paired comparison *t*-test). These results confirm previous reports that postreceptoral activity from the Off pathway was greatly affecting the leading edge of the a-wave at the time of the trough of the a-wave in normal mouse eyes (Maeda et al., 2003; Sharma et al., 2005).

Light-adapted ERG response to long flashes

In order to see whether the positive intrusion occurred at light offset, as expected for a response generated by the Off pathway, the stimulus duration was lengthened to allow separation of On and Off responses. Fig. 5A shows typical light-adapted ERGs of *Nob* mice in response to brief (< 4 ms) and longer duration (200 ms) stimuli. The typical long flash response of the *Nob* ERG was predominantly negative-going, with a small positive intrusion occurring after stimulus offset.

Fig. 5B shows the long flash response from Fig. 5A on an expanded time scale in order to assess the timing of the positive intrusion at light offset. The positive intrusion of the long-flash ERG started about 20 ms after the stimulus offset, and it had a similar time course to the response to brief flashes, reaching a peak around 70 ms later. These times were similar for all *Nob* mice across stimulus energies. A positive-going response in the ERG at light offset is generally called a d-wave. However, the slow time to peak in the mouse distinguishes it from d-waves recorded in other species such as humans and monkeys where it rises to a peak rapidly (e.g. Sieving et al., 1994). This peak was not obvious in Control mice before APB injection (see inset to Fig. 5B).

The amplitudes of the ERG at the onset of the positive intrusion in the long-flash response (220 ms) and at the peak of the positive intrusion (290 ms) are shown in Fig. 5C, middle panel for four *Nob* mice. For comparison measurements from the brief-flash ERG from Fig. 2C are included in the left hand panel. The positive intrusion of the long flash ERG (shaded area) was larger on average than that in the brief flash ERG for the strongest stimuli, but this was not significant, due to high variability. Injection of PDA eliminated the positive intrusion as shown

by the dashed line in Fig. 5B (left) for one animal, and by the similarity in response amplitude at 220 ms and 290 ms after PDA for all the animals in Fig. 5C, right hand plot, Similar results were observed in Control APB long-flash responses before and after PDA injection (data not shown).

Comparison of young and old *Nob* mice in response to brief-flash stimuli

A few *Nob* mice that were about one year of age were present in our colony. We repeated the experiments that we had done on the younger *Nob* mice with brief flashes, described above, to see if the advanced age of these animals would affect their ERGs, as compared to ERGs of young Nob mice or similarly old Control APB mice. The middle column in Fig. 6A shows ERGs of old *Nob* mice in response to brief flashes of increasing stimulus energy. For comparison, the responses of a typical young *Nob* mouse from Fig. 1 are shown in the left hand column. In Fig. 6D, responses from an old and young mouse to the strongest stimulus are superimposed. The negative going response was smaller in the old *Nob* ERG than in the young *Nob* ERG, but the positive intrusion looked similar for the two mice.

The plots in Fig. 6F of averages from six young and six old *Nob* mice confirm that the positive intrusion measured between 50 and 120 ms after the flash was similar in amplitude for all stimulus energies for the two groups ($P>0.05$, two sample *t*-test with unequal variance for all statistics in this section). However, the response measured at 50 ms after the flash was much smaller in the old *Nob* mice than in the young *Nob* mice for the four strongest stimuli ($P<.05$); it was maximally about half the amplitude of the young *Nob* ERG.

Fig. 6C illustrates the ERG of the old *Nob* mouse ERG after PDA for the mouse whose responses are illustrated in part B. As in the young *Nob* mice, PDA eliminated the positive intrusion. Fig. 6F, right hand plot shows that the average data support this observation. The average data also show that maximum negative response for the strongest stimulus, measured at 50 ms was about half of that before PDA, as had been observed for the young *Nob* mice (Fig. 2D).

Fig. 6E shows measurements of a-wave amplitude at the trough time found for control ERGs (15 ms after the flash) in response to brief flashes of increasing stimulus energy. Interestingly, when measured at 15 ms, the old *Nob* and young *Nob* responses showed almost the same negative amplitude for all stimulus energies that were tested. The old *Nob* a-waves after PDA injection (measured at 15 ms) were greatly reduced compared to those before PDA injection ($P< 0.003$, paired comparison *t*-test, for 1.3 log sc td s, and much less for higher stimulus energies). The reduction was slightly more than that seen in Fig. 4 for young mice.

ERGs of two Control mice (4 eyes) that also were about a year old were measured after APB injection.. The amplitude of the negative response was reduced relative to typical young mice, but in each eye of each animal by about 25%, rather than by 50% seen in *Nob* mice. Measurements from the right eyes of the two mice are illustrated in the inset to Fig. 6 F, middle panel. The amplitudes were measured at 40 ms and 100 ms as in Fig. 2D for young Controls, and in each case almost 60 of the 80 μV measured in young animals at 40 ms was still present. The size of the positive intrusion in Control APB old mice was similar to that in young animals, as was observed for the *Nob* mice. The number of Control eyes was small, and these findings are not conclusive, but they suggest more severe aging effects in *Nob* mice than in control mice.

ERG responses to sinusoidal stimulation (Flicker ERG)

Up to this point experiments using flashed stimuli have been described to evaluate postreceptoral cone pathway function in *Nob* mice. In this section, we describe flicker ERG responses of *Nob* and Control mice, as an alternative way to evaluate cone pathway function.

Fig. 7 shows typical flicker ERG responses of Control and *Nob* mice. The control responses (Fig. 7A) had markedly higher amplitudes than the *Nob* responses (Fig. 7B). (A). Therefore, we confirm, as reported previously (Krishna et al., 2001) that the On pathway in normal mice contributes significantly to the mouse flicker ERG. However, a small contribution from the Off pathway, much of which could be removed by injection of PDA (right hand column), also was apparent.

In order to compare the temporal phase of the *Nob* and control responses, in Fig. 7D and E, flicker ERG responses with amplitudes all scaled to be equal were superimposed. Three periods are shown for each temporal frequency of stimulation (3, 9 and 15 Hz) to facilitate seeing the phase differences across the three groups: Control, *Nob*, and *Nob* PDA. Phases were similar for *Nob* and *Nob* PDA animals in all records. Phase differences between Control and *Nob* mice, (or Control and *Nob* PDA mice) were more than 180° at 3 Hz, at 9 Hz they were about 180° and at 15 Hz they were quite small.

A phase difference of 180° would be consistent with the loss of the On pathway contribution in *Nob* animals (also see Krishna et al., 2002). The amplitude and phase difference between Control and *Nob* animals, and between *Nob* and *Nob* PDA animals are explored further in Fig. 8.

Fig. 8 shows plots of flicker ERG amplitudes and phases versus temporal frequency for three control and three *Nob* mice. Analysis of 2^{nd}-harmonic responses (F2), as well as responses to the fundamental frequency (F1) of stimulation, are included in the figure. F2 responses are thought to be generated mostly by inner retina, i.e. amacrine and ganglion cells, at least in primate subjects (Viswanathan et al., 2002). The F1 amplitude of control mice was about 70 μV at its peak frequency of 8 Hz, while for *Nob* mice, it was less than 20 μV at its slightly lower peak frequency of 5 – 6 Hz. After the PDA injection in *Nob* mice, when postreceptoral influences presumably were removed, the largest response amplitude was about 10μV at 3 Hz, the lowest frequency tested, and it declined steady as frequency increased. The F1 response could be recorded up to 21 Hz in control and *Nob* mice and 15 Hz in *Nob* PDA mice. At 3 Hz, F1 phase was about 270° more delayed in *Nob* than in control mice, and the difference declined to zero by 12 Hz. As noted above, phase was not altered appreciably by PDA.

The F2 frequency response showed two amplitude peaks in control mice, one at 3 Hz (or lower) and one at 17 Hz. The F2 peak amplitude was much lower than the F1 peaks, being around 10 μV for the high frequency. The amplitude of the *Nob* F2 responses was very low, less than 3 μV for frequencies up to 12 Hz, with no high frequency peak at 17 Hz. *Nob* ERGs following PDA injection showed almost no F2 response. The phase delay of the Control responses increased at a higher rate with temporal frequency than delay for the F1 responses. Phase measurements plotted when responses were small to negligible in *Nob* and *Nob* PDA reecords were based on noise, as can be seen by noise levels plotted in the amplitude plots.

Postreceptoral contribution to the sinusoidal flicker ERG in *Nob* mice

In the light-adapted flash ERG of *Nob* mice, it was possible to measure the amplitude of the positive intrusion that was generated from postreceptoral cells directly. However, the extent to which postreceptoral cells contribute to the *Nob* flicker ERG is less straight forward because both amplitude and phase must be taken into account. If we simply calculate the difference between *Nob* and *Nob* PDA fundamental amplitudes, the difference will be much smaller than

the actual difference, especially for the low temporal frequencies. We therefore attempted to quantify the postreceptoral contribution to the *Nob* flicker ERG by using vector analysis as done previously by Kondo et al.(2001) for macaque flicker ERG..

To quantify the contribution of the postreceptoral cells we derived the vector difference between the fundamental response of *Nob* and that of *Nob* after PDA injection. Examples of the vector subtraction analysis for temporal frequencies of 3 Hz, 6 Hz, and 9 Hz are shown in Fig. 9. The phase delays for the *Nob* and *Nob* after PDA data, which increased as temporal frequency was increased, were acquired from the plot in Fig. 8B.

Fig. 10 shows a plot of average fundamental amplitude vs. temporal frequency for the *Nob*, the *Nob* PDA data and the *Nob* postreceptoral response that was derived from vector analysis. From this figure it is clear that the postreceptoral component dominates the F1 amplitude in the *Nob* flicker ERG, except at low frequencies, and frequencies above 30 Hz. Given the similarity of the flash ERG results and the difficulty of the Control APB experiments, flicker experiments were not done for Control APB animals.

Isolation and time course of cone photoreceptor-driven responses

In experiments in which PDA was used to remove residual postreceptoral activity in the ERGs of mice lacking b-waves, the remaining response should have depended solely upon the activation of the cone photoreceptors. However, as can be seen in Fig. 2A and 2B for responses to a brief flash of 2.5 log sc td s for example, the response peak was quite delayed, occurring about 90 ms after the flash, and the response did not recover to baseline for at least 600 ms (see Fig. 3). M-cone photoreceptor currents, recorded from mouse outer segments are observed to peak around 70 ms after a weak flash and to recover to baseline in around 200 ms (Nikonov et al., 2006). Times to peak for stronger flashes such as we used would be earlier. Because a rod saturating background was used, it was unlikely that the slowly recovering responses in the present study were rod-driven, although the time course is more reminiscent of rods than cones. The slow response suggests the presence of a Müller cell, negative-going slow PIII response, and (possibly smaller) retinal pigment epithelium positive-going c-wave response of similar time course (Wu et al., 2004). These slow responses, well-documented in the dark-adapted ERG, occur in response to changes in the extracellular potassium concentration in the subretinal spaced mainly as a consequence of interruption of the rod photocurrent (e.g. Steinberg et al., 1980). Given this possibility, it was important to isolate the photoreceptor responses from other photoreceptor-dependent signals.

The approach adopted was one originally described by Pepperberg et al. (1997) for isolating rod photoreceptor responses in humans, and subsequently adapted for use in mice (Hetling and Pepperberg, 1999; Kang Derwent et al., 2007). Guidance for studying cone responses which are smaller in amplitude and of shorter time course than rod responses was found in the work of Friedburg et al. (2004) in humans, and Daniele et al. (2005) in mice. In the presnt study, a brief test flash was presented on the standard rod-saturating background and was followed at a range of intervals during the test flash response by a probe flash that was intense enough to turn off the cone-circulating current. The a-wave produced by probe flash after the test flash was smaller than that of probe flash alone, because the test flash has already consumed some of the cone-circulating current. The difference between the response to the test plus probe and probe alone yielded the cone-circulating current at the tested time points after test flash onset, which, when subtracted from the response to the probe flash alone, could be used to map out the time course of the cone photoreceptor response. The amplitudes were measured on the leading edge of the a-wave at 8 ms after the flash, which was still likely to be a cone photoreceptor response, according to experiments in Fig. 4 showing effects of PDA on the a-wave only after about 8 to 10 ms for a stimulus of 2.5 log sc td s. The amplitude of the derived

response would be smaller than its contribution to the recorded flash ERG, due to being measured at early times before the maximum amplitude of the response.

Fig. 11 shows average derived cone responses using the paired flash technique for three *Nob* recordings (Fig. 11A, two eyes from one mouse), and for three Control mice (Fig 11B) for a brief-flash stimulus of 2.5 log sc td s. For comparison, Fig 11 C and D shows average flash ERGs for the same stimulus for *Nob* mice injected with PDA and for Control APB mice injected with PDA to remove postreceptoral contributions. The derived (isolated) cone responses in parts A and B were of much shorter duration than the recorded ERG waveforms in parts C and D. The derived response to this moderately strong stimulus reached a peak between 23 and 33 ms (time points that were tested) after the flash, and returned to baseline within 200 ms. A similar time course was found for derived responses to flashes that were four times weaker, when recorded brief flash ERGs recovered in 400–500 ms (data not shown). These findings are consistent with the interpretation that the long-lasting negative ERG waves that were recorded from *Nob* PDA and Control APB+PDA were formed not only by cone photoreceptor currents, but also by photoreceptor-dependent signals from other retinal elements, probably Müller and perhaps RPE cells.

DISCUSSION

The main purpose of the present study was to determine the extent to which postreceptoral neurons in the Off pathway contribute to the light-adapted ERG of the *Nob* mouse. The normal mouse ERG, unlike the human ERG, does not show a positive-going d-wave at light offset, which has been puzzling because there are functional On and Off circuits in the mouse retina, as in other mammals that have obvious d-waves. Therefore the *Nob* mouse, which does not generate an ERG b-wave provided an opportunity to study ERGs where any postreceptoral contribution would necessarily originate from the Off pathway. In this study, postreceptoral neurons from the Off pathway were found to make a significant positive-going contribution, which we called a “positive intrusion”, to the flash ERG response of *Nob* mice, as well as to the ERG of Control mice injected with APB to remove On pathway activity. Postreceptoral neurons also were found to provide a substantial proportion of the *Nob* mouse light-adapted ERG response to sinusoidally modulated stimuli.

The positive intrusion

Regardless of stimulus duration, the ERG of the *Nob* mouse was predominantly negative-going, although it had a small, late, positive intrusion in the response to brief flashes, and a positive intrusion at light offset in response to longer duration flashes.

In order to see whether the response was unique to the *Nob* mice, or it existed in normal (Control) eyes with On-pathway activity eliminated, the *Nob* ERG in this study was compared to the ERG in normal eyes of C57BL/6 mice injected intravitreally with APB. Positive intrusions were qualitatively similar in the two different models that lacked On pathway function, although the positive intrusion for the brief stimuli was larger, started earlier, and peaked slightly earlier (by ~ 10 ms) in Control APB eyes than in *Nob* eyes. Positive intrusions of amplitudes more similar to Control APB than *Nob* mice have recently been reported in mGluR6-deficient mice as well (Koyasu et al., 2008). The reason for these difference is unclear, but may indicate abnormalities in postreceptoral Off pathway activity of *Nob* mice. In fact, in extracellular recordings from Off ganglion cells in *Nob* mice, activity has been observed to be abnormal (Demas et al., 2006; Gregg et al., 2007). Importantly however, both in *Nob* mice and Control mice injected with APB the positive intrusion was completely removed (see Figs. 2, 3, 5 and 6) by PDA which blocked the light-evoked Off pathway activity originating from second order (Off bipolar, or horizontal cells, and third order neurons (amacrine and ganglion cells) (Slaughter and Miller, 1993; Massey, 1990 for review). PDA also removed the positive

wave in mGLur6-deficient mice (Koyasu et al., 2008). Preliminary experiments with pharmacological agents that primarily interfere with signaling in the inner retina, e.g. tetrodotoxin to block sodium-dependent spiking activity, and n-methyl D- aspartate (NMDA) (e.g. Robson and Frishman, 1995) or GABA (Robson et al., 2004) to minimize inner retinal contributions to the ERG, indicate that the positive intrusion originates at least in part from neurons proximal to Off bipolar cells (unpublished observations). Additional experiments would be needed to further specify the third order contributions to the response.

Relation of the positive intrusion to the d-wave—The positive-going wave in the ERG at light offset is generally called the d-wave. Despite the slower time course of the d-wave in *Nob* mice than in animals where it is readily seen (e.g. macaque), the positive intrusion at offset of a long duration flash is the only positive-going response present and can be viewed as being the mouse d-wave.

Pharmacologic blockade studies in macaque retina have shown that the d-wave originates primarily from a combination of the positive-going offset of cone photoreceptor responses, and depolarization of the Off bipolar cells at light offset (Sieving et al., 1994; Uneo et al., 2006). In addition, there are small contributions from third order neurons, and an opposing wave from the negative-going offset of the b-wave (repolarization of On bipolar cells) that pulls the response down, i.e. the d-wave is larger in normal macaque eyes when APB is injected intravitreally to eliminate light-driven On cone bipolar activity (Uneo et al., 2006). The presence of a strong opposing influence in normal mouse eyes from the On pathway may explain why the “d-wave” is not seen in those eyes. Removal of On pathway influence in *Nob* mice or by APB injection was needed to see the small d-wave.

A positive intrusion in the brief-flash ERG can be prominent in macaque eyes injected with APB (Bush and Sieving, 1994). As in the *Nob* mice and Control mice injected with APB, the intrusion can also be eliminated by injection of PDA in macaque eyes. The intrusion in the brief-flash ERG of the macaque, like the d-wave, is faster in onset and peak time than in the mouse ERG (Bush and Sieving, 2004). It is likely that it manifests as PDA-sensitive i-wave in the normal primate ERG (Rangaswamy et al., 2004). Responses in the cone system are generally faster in primates than in mice, as addressed more thoroughly in a later section on photoreceptor responses.

Relative timing of the positive intrusion in the brief- vs. long-flash ERG in *Nob* mice—The positive intrusion of long-flash ERG in *Nob* mice started about 20 ms after the stimulus offset (Fig. 5B), whereas it occurred much later, 50 ms, relative to *onset* of the brief flash. We can regard the brief flash (lasting <4 ms) essentially as a combination of an onset-stimulus and offset-stimulus, meaning that the Off bipolar cell would hyperpolarize for some minimal response duration, and then depolarize in response to the brief stimulus. In contrast, in the in the case of the offset of a long flash, Off bipolar cell responses would already be hyperpolarized, so they would only depolarize in response to stimulus offset. This may explain why the positive intrusion after the long flash started earlier than that of short flash.

Effect of PDA on the a-wave

As previously described for primates, as well as for mice, Off pathway activity contributes to the leading edge of the a-wave under light-adapted conditions quite early in the response (Bush and Sieving, 1994; Robson et al., 2003; Maeda et al., 2003; Ohtoshi et al., 2004; Sharma et al., 2005). In the present study Fig. 4A shows that PDA began to alter the leading edge of the a-wave around 8–10 ms after the flash, consistent with other mouse studies from this lab (Maeda et al., 2003; Ohtoshi et al., 2004). In macaques effects of intravitreal PDA injection can be seen as early as 5 ms after a brief flash (Robson et al., 2003). In Figs. 2, 4 and 6 in the present study

it can be seen that the negative potential that PDA eliminated peaked around 50 ms after the flash in *Nob* mice (slightly earlier in Control APB mice). The early contributions to the a-wave are probably dominated by hyperpolarizing (Off) bipolar cells, and later contributions may also include activity of third order neurons in the Off pathway (Maeda et al., 2003; Sharma et al., 2005), The role of the horizontal cells, if any, is unresolved.

Effects of PDA on the dark-adapted a-wave of normal and *Nob* mouse also have been studied. In a recent study in this lab (Kang Derwent et al., 2007), effects of PDA were found to be insignificant when the leading edge of the saturated rod-driven a-wave was measured around 6 ms after the flash. However, for less saturated a-waves with slower onset and time to peak, reductions in a-wave amplitude measured at later times in the response were observed after PDA injection in *Nob* mice, and Control mice injected with APB (unpublished observations).

Photoreceptor contributions to the mouse light-adapted ERG

The brief-flash light-adapted ERG responses of *Nob* mice after PDA injection and Control mice after APB + PDA injection to remove postreceptoral contributions to the ERG was composed of a negative wave that peaked 90 ms after the flash, and lasted about 600 ms for a moderately strong stimulus of 2.5 log sc td s that produced a nearly maximal b-wave. This duration is very prolonged compared to results from suction electrode recordings from mouse M-cones. In suction electrode recordings, outer segment currents were reduced only for about 200 ms for weak stimuli, with a peak reduction around 70 ms after a brief flash (Nikonov et al., 2006). In the present study, in order to isolate the cone photoreceptor contribution to the ERG, the paired flash approach (Pepperberg et al., 1997) was used to derive the photocurrent. The derived cone-photoreceptor responses in the *Nob* and C57BL/6 mice ERGs were found to peak between 23 and 33 ms after a brief flash, and to recover in about 200 ms in response to a moderately strong stimulus of 2.5 log sc td s (see Fig. 11). The peak time of the derived response was probably earlier than that found in the suction electrode recordings for a couple of reasons: first the flash was stronger in our experiments, and responses to strong flashes peak sooner. Second, derived photoreceptor responses are generally found to be faster than responses in suction electrode recordings, probably because of the more physiological recording conditions. For example, photocurrents recorded from macaque monkey outer segments were found to peak at 54 ms (Schnapf et al., 1990). However, cone photoreceptor responses to dim and moderate energy flashes measured in human, derived by the paired flash ERG technique, peak around 20 ms after a brief flash and last about 100 ms (Friedburg et al., 2004; van Hateren and Lamb, 2006). Comparing species, cone photocurrents recorded with suction electrodes and derived cone responses both are slower in mice than in primates, which is consistent with the poorer temporal resolution observed in the photopic flicker ERGs in mice compared to primates (e.g. Krishna et al., 2001; Viswanathan et al., 2002, and the present study).

The explanation for the prolonged negative response in the ERG of mice lacking postreceptoral responses is that in addition to the cone photoreceptor, the response also includes negative-going slow Plll and perhaps some positive-going c-wave from the RPE. Slow PIII reflects potassium currents in Müller cells, induced by changes in extracellular potassium when photoreceptors hyperpolarize, that affect inward rectifying potassium channels on the Müller cells (Kofuji et al., 2002: 2004; Wu et al., 2004), as well as the pigment epithelium. The initial effect on the light-adapted ERG was to augment the negative-going response, indicating a initially larger slow PIII than the c-wave.

It is a little surprising that a slow potassium-dependent response was so prominent in light-adapted responses. They are more commonly observed under dark-adapted conditions in mammals (e.g. Steinberg et al., 1980). It may also seem surprising that slow PIII began to affect the response as early as 30 ms after flash with a peak effect at 90 ms. We have observed a similar time course for slow PIII under dark-adapted conditions in response to high energy

flashes (unpublished observations). Under dark-adapted conditions, however, the slow PIII contribution and the derived rod photoreceptor response have a similar peak time around 90 ms (unpublished observations).

Effects of aging on the light-adapted ERG of mice lacking b-waves

Amplitudes of light-adapted ERGs of *Nob* mice were affected by aging in this study (Fig. 6). Effects on Control APB mice were much smaller. In previous studies by other investigators, the amplitudes of dark-adapted a-waves and b-wave were found to be reduced as mice aged for both C57BL/6 mice (pigmented mice) and Balb/c mice (albino mice) (Gresh et al., 2003;Li et al., 2001). Between four and 17 months of age, there was a substantial loss of rod photoreceptors (more in the albino mice), which contributed to the reduced ERG amplitudes. But aging effects have been less obvious for cones, whose counts (middle wavelength) were reduced in aged Balb/c mice, but not in C57BL/6 mice (Gresh et al., 2003;Jacobs and Williams, 2007;Li et al., 2001). Cone-driven flash ERGs were found to be reduced in mice that are a year old, and light-adapted flicker ERG amplitudes were affected, but only mildly in the pigmented mice (Jacobs et al., 2007;Li et al., 2001). The findings in the present study for one year old *Nob* mice versus three to six month old mice show no change in cone photoreceptor driven a-waves measured at 6 or 8 ms after a brief flash, and no change in the amplitude of the positive intrusion. The major effect was on the postreceptoral portion of the a-wave, and the very slow portion of the response, whose time course is controlled by addition of a negative-going slow PIII and perhaps some positive going RPE C-wave (see above). This finding raises the possibility that aging effects on postreceptoral elements, and Müller cell function may be more pronounced than on some other retinal elements, particularly in *Nob* mice. An additional consideration is that the slow negative wave may reflect rod-related signals, and rods are known to be more affected in aging mouse eyes than cones (Gresh et al., 2005; Li et al., 2001). While we cannot completely eliminate this possibility, the backgrounds that we used, have been used in numerous other studies to suppress rod activity.

Postreceptoral contributions to sinusoidal flicker ERG in *Nob* mice

In this study we confirmed and extended observations of Krishna et al. (2003) on the flicker ERG in the *Nob* mouse. As they reported, *Nob* flicker ERGs are much smaller in amplitude, and reversed in phase compared to flicker ERGs of normal eyes. Changes in phase are a characteristic of complete type CSNB in humans as well (Kim et al., 1997). In this study we discovered that the residual tuning of the response, with a peak around 6 Hz, is due to postreceptoral contributions that can be eliminated by PDA. After injection of PDA the function relating response amplitude and temporal frequency became low pass, with the largest response at the lowest frequency tested. This low pass characteristic reflects the slow time course of the response, thought to be due to the presence of slow PIII and the C-wave. However, even if these slower contributions were not present, the response amplitudes would be too low to produce tuning to some higher frequency. The full extent of the postreceptoral contribution to the *Nob* mouse ERG, was demonstrated only when vector analysis was used to display the component, as was done previously in for macaque ERG for separating On and Off pathway contributions (Kondo et al., 2001).

The present study also extended previous findings by examining second harmonic responses in the *Nob* sinusoidal flicker ERG. Second harmonic responses have been shown in pharmacological blockade experiments in macaque, to contain considerable contributions from (spiking) inner retinal neurons (e.g. Viswanathan et al., 2002), and similar observations have been made in mouse (our unpublished observations). For low temporal frequencies, the response was reduced by about the same proportion as the F1 response. In contrast, the high frequency peak around 17 Hz in normal eyes, was completely eliminated. It is possible that

both On and Off pathway inner retinal activity are necessary to generate second harmonic responses, or On pathway may be more important than the Off pathway for the response.

Future perspective

This investigation of ERGs lacking b-waves provides further insights about Off pathway contributions to the mouse ERG. These insights and the approach that was used to acquire them may be of value as more murine models for human retinal disease emerge.

Acknowledgements

This work was supported by National Eye Institute Grants R01-EY06671, P30-EY07751.

References

Ball SL, Pardue MT, McCall MA, Gregg RG, Peachey NS. Immunohistochemical analysis of the outer plexiform layer in the *nob* mouse shows no abnormalities. Vis Neurosci 2003;20:267–272. [PubMed: 14570248]

Bech-Hansen NT, Naylor MJ, Maybaum TA, Sparkes RL, Koop B, Birch DG, Bergen AA, Prinsen CF, Polomeno RC, Gal A, Drack AV, Musarella MA, Jacobson SG, Young RS, Weleber RG. Mutations in NYX, encoding the leucine-rich proteoglycan nyctalopin, cause X-linked complete congenital stationary night blindness. Nat Genet 2000;26:319–323. [PubMed: 11062471]

Bergen AA, ten Brink JB, Riemslag F, Schuurman EJ, Meire F, Tijmes N, de Jong PT. Conclusive evidence for a distinct congenital stationary night blindness locus in Xp21.1. J Med Genet 1996;33:869–872. [PubMed: 8933343]

Boycott KM, Pearce WG, Musarella MA, Weleber RG, Maybaum TA, Birch DG, Miyake Y, Young RS, Bech-Hansen NT. Evidence for genetic heterogeneity in X-linked congenital stationary night blindness. Am J Genet 1998;62:865–875.

Bush RA, Sieving PA. A proximal retinal component in the primate photopic ERG a-wave. Invest Ophthalmol Vis Sci 1994;35:635–645. [PubMed: 8113014]

Bush RA, Sieving PA. Inner retinal contributions to the primate photopic fast flicker electroretinogram. J Opt Soc Am A 1996;13:557–565.

Candille SI, Pardue MT, McCall MA, Peachey NS, Gregg RG. Localization of the mouse *nob* (no b-wave) gene to the centromeric region of the X chromosome. Invest Ophthalmol Vis Sci 1996;40:2748–2751. [PubMed: 10509675]

Daniele LL, Lillo C, Lyubarsky AL, Nikonov SS, Philp N, Mears AJ, Swaroop A, Williams DS, Pugh EN Jr. Cone-like morphological, molecular, and electrophysiological features of the photoreceptors of the Nrl knockout mouse. Invest Ophthalmol Vis Sci 2005;46:2156–2167. [PubMed: 15914637]

Demas J, Sagdullaev BT, Green E, Jaubert-Miazza L, McCall MA, Gregg RG, Wong RO, Guido W. Failure to maintain eye-specific segregation in *nob*, a mutant with abnormally patterned retinal activity. Neuron 2006;50:247–259. [PubMed: 16630836]

Dryja TP, McGee TL, Berson EL, Fishman GA, Sandberg MA, Alexander KR, Derlacki DJ, Rajagopalan AS. Night blindness and abnormal cone electroretinogram ON responses in patients with mutations in the GRM6 gene encoding mGluR6. Proc Na'l Acad, Sci USA 2005;102:4884–4889.

Friedburg C, Allen CP, Mason PJ, Lamb TD. Contribution of cone photoreceptors and post-receptoral mechanisms to the human photopic electroretinogram. J Physiol 2004;556:819–834. [PubMed: 14990682]

Gregg RG, Kamermans M, Klooster J, Lukasiewicz PD, Peachey NS, Vessey KA, McCall MA. Nyctalopin expression in retinal bipolar cells restores visual function in a mouse model of complete X-linked congenital stationary night blindness. J Neurophysiol 2007;98:3023–3033. [PubMed: 17881478]

Gregg RG, Mukhopadhyay S, Candille SI, Ball SL, Pardue MT, McCall MA, Peachey NS. Identification of the gene and the mutation responsible for the mouse *nob* phenotype. Invest Ophthalmol Vis Sci 2003;44:378–384. [PubMed: 12506099]

Gresh J, Goletz PW, Crouch RK, Rohrer B. Structure-function analysis of rods and cones in juvenile, adult, and aged C57BL/6 and Balb/c mice. Vis Neurosci 2003;20:211–220. [PubMed: 12916741]

Hetling JR, Pepperberg DR. Sensitivity and kinetics of mouse rod flash responses determined in vivo from paired-flash electroretinogram. J Physiol 1999;516:593–609. [PubMed: 10087356]

Jacobs GH, Williams GA. Cone-based vision in the aging mouse. Vision Res 2007;47:2037–2046. [PubMed: 17509638]

Jacobs GH, Williams GA, Fenwick JA. Influence of cone pigment coexpression on spectral sensitivity and color vision in the mouse, Vis. Res 2004;44:1615–1622.

Jamison JA, Bush RA, Lei B, Sieving P. Characterization of the rod photoresponse isolated from the dark-adapted primate ERG. Vis Neurosci 2001;18:445–455. [PubMed: 11497421]

Kang Derwent JJ, Saszik SM, Maeda H, Little DM, Pardue MP, Frishman LJ, Pepperberg DR. Test of the paired flash electroretinographic method in mice lacking b-waves. Vis Neurosci 2007;24:141–149. [PubMed: 17640404]

Kaneko M, Maeda H, Frishman LJ. Effects of prolonged light adaptation on the amplitude of the A-wave of the flash ERG of the mouse. ARVO E-Abstracts, #3095. 2006

Khan NW, Kondo M, Hiriyanna KT, Jamison JA, Bush RA, Sieving PA. Primate retinal signaling pathways: Suppressing ON-pathway activity in monkey with glutamate analogs mimics human CSNB1-NYX genetic night blindness. J Neurophysiol 2005;93:481–492. [PubMed: 15331616]

Kim SH, Bush RA, Sieving PA. Increased phase lag of the fundamental harmonic component of the 30 Hz flicker ERG in Schubert-Bornschein complete type CSNB. Vis, Res 1997;37:2471–2475. [PubMed: 9381682]

Knapp AG, Schiller PH. The contribution of on-bipolar cells to the electroretinogram of rabbits and monkeys: A study using 2-amino-4-phosphonobutyrate (APB). Vis Res 1984;24:1841–1846. [PubMed: 6534006]

Kofuji P, Biedermann B, Siddharthan V, Raap M, Iandiev I, Milenkovic I, Thomzig A, Veh RW, Bringmann A, Reichenbach A. Kir Potassium channel subunit expression in retinal grail cells: Implications for spatial potassium buffering. Glia 2002;39:292–303. [PubMed: 12203395]

Kofuji P, Ceelen P, Zahs KR, Surbeck LW, Lester HA, Newman EA. Genetic inactivation of an inwardly rectifying potassium channel (Kir4.1 Subunit) in mice: Phenotypic impact in retina. J Neurosci 2000;20:5733–5740. [PubMed: 10908613]

Kondo M, Sieving PA. Primate photopic sine-wave flicker ERG: Vector modeling analysis of component origins using glutamate analogs. Invest Ophthalmol Vis Sci 2001;42:305–312. [PubMed: 11133883]

Koyasu T, Kondo M, Miyata K, Ueno S, Miyata T, Nishizawa Y, Terasaki H. Photopic electroretinograms of mGluR6-Deficient Mice. Curr Eye Res 2008;33:91–99. [PubMed: 18214746]

Krishna VR, Alexander KR, Peachey NS. Temporal properties of the mouse cone electroretinogram. J Neurophysiol 2002;87:42–48. [PubMed: 11784728]

Li C, Cheng M, Yang H, Peachey NS, Naash MI. Age-related changes in the mouse outer retina. Optom Vis Sci 2001;78:425–430. [PubMed: 11444632]

Lyubarsky AL, Pugh EN Jr. Recovery phase of the murine rod photoresponse reconstructed from electroretinographic recordings. J Neurosci 1996;16:563–571. [PubMed: 8551340]

Maeda H, Saszik SM, Frishman LJ. Postreceptoral Contributions to the a-wave of the photopic flash ERG of the mouse retina. ARVO E-Abstract #1891. 2003

Massey, SC. Cell types using glutamate as a neurotransmitter in the vertebrate retina. In: Osborne, N.; Chader, G., editors. Prog in Ret Res. 9. Pergamon Press; Oxford: 1990. p. 399-425.

Miyake Y, Yagasaki K, Horiguchi M, Kawase Y, Kanda T. Congenital stationary night blindness with negative electroretinogram. Arch Ophthalmol 1986;104:1013–1020. [PubMed: 3488053]

Miyake, Y.; Yagasaki, K.; Horiguchi, M.; Kawase, Y. Jpn J Ophthalmol. 31. 1987. On- and Off-responses in photopic electroretinogram in complete and incomplete types of congenital stationary night blindness; p. 81-87.

Naarendorp F, Sieving PA. The scotopic threshold response of the cat ERG is suppressed selectively by GABA and glycine. Vis Res 1991;31:1–15. [PubMed: 2006543]

Nikonov SS, Kholodenko R, Lem J, Pugh EN Jr. Physiological features of the S-and M-cone photoreceptors of wild-type mice from single-cell recordings. J Gen Physiol 2006;127:359–374. [PubMed: 16567464]

Ohtoshi A, Wang SW, Maeda H, Saszik SM, Frishman LJ, Klein WH, Behringer RB. Regulation of cone bipolar cell differentiation and photoptic vision by the CVC homeobox gene vsx1. Curr Biol 2004;14:530–536. [PubMed: 15043821]

Pardue MT, McCall MA, LaVail MM, Gregg RG, Peachey NS. A naturally occurring mouse model of X-linked congenital stationary night blindness. Invest Ophthalmol Vis Sci 1998;39:2443–2449. [PubMed: 9804152]

Peachey NS, Alexander KR, Fishman GA. Visual adaptation and the cone flicker electroretinogram. Invest Ophthalmol Vis Sci 1991;32:1517–1522. [PubMed: 2016133]

Pesch K, Zeitz C, Fries JE, Munscher S, Pusch CM, Kohle RK, Berger W, Wissinger B. Isolation of the mouse nyctalopin gene nyx and expression studies in mouse and rat retina. Invest Ophthalmol Vis Sci 2003;44:2260–2266. [PubMed: 12714669]

Pinto LR, Vitaturna MA, Shimomura K. Generation, identification and functional characterization of the *Nob*4 mutation of GRM6 in the mouse. Vis Neurosci 2007;24:111–123. [PubMed: 17430614]

Pepperberg DR, Birch DG, Hood DC. Photoresponses of human rods in vivo derived from paired-flash electroretinograms. Visual Neurosci 1997;14:73–82.

Robson JG, Frishman LJ. Response linearity and dynamics of the cat retina: the bipolar cell component of the dark-adapted ERG. Visual Neurosci 1995;12:837–850.

Robson JG, Saszik SM, Ahmed J, Frishman LJ. Rod and cone contributions to the a-wave of the electroretinogram of the macaque. J Physiol 2003;547:509–530. [PubMed: 12562933]

Rozzo C, Fossarello M, Gallei G, Miano MG, Ciccodicola A, Sole G, Pirastu M. Complete congenital stationary night blindness maps on Xp11.4 in a Sardinian family. Eur J Hum Genet 1999;7:574–578. [PubMed: 10439964]

Saszik SM, Robson JG, Frishman LJ. The scotopic threshold response of the dark-adapted electroretinogram of the mouse. J Physiol 2002;543:899–916. [PubMed: 12231647]

Schnapf JL, Nunn BJ, Meister M, Baylor DA. Visual transduction in cones of the monkey Macaca fascicularis. J Physiol 1990;427:681–713. [PubMed: 2100987]

Sharma S, Ball SL, Peachey NS. Pharmacological studies of the mouse cone electroretinogram. Vis Neurosci 2005;22:631–636. [PubMed: 16332274]

Shirato S, Maeda H, Frishman LJ. Postreceptoral contributions to the photopic ERG of *Nob* mice. ARVO E-Abstracts, #2254. 2005

Sieving PA, Murayama K, Naarendorp F. Push-pull model of the primate photopic electroretinogram: A role for hyperpolarizing neurons in shaping the b-wave. Vis Neurosci 1994;11:519–532. [PubMed: 8038126]

Slaughter MM, Miller RF. 2-amino-4-phosphonobutyric acid: a new pharmacological tool for retina research. Science 1981;211:182–185. [PubMed: 6255566]

Slaughter MM, Miller RF. Bipolar cells in the mudpuppy retina use an excitatory amino acid neurotransmitter. Nature 1983;303:537–538. [PubMed: 6134238]

Steinberg RH, Oakley B 2nd, Niemeyer G. Light-evoked changes in [K+]0 in retina of intact cat eye. J Neurophysiol 1980;44:897–921. [PubMed: 7441322]

Tsukamoto Y, Morigiwa K, Ueda M, Sterling P. Microcircuits for night vision in mouse retina. J Neurosci 2001;21:8616–8623. [PubMed: 11606649]

Ueda Y, Tammitsu N, Imai H, Honda Y, Shichida Y. Recovery of rod-mediated a-wave during light-adaptation in mGluR6-deficient mice. Vis Res 2006;46:1655–1664. [PubMed: 16243375]

Ueno S, Kondo M, Ueno M, Miyata K, Terasaki H, Miyake Y. Contribution of retinal neurons to d-wave of primate photopic electroretinograms. Vision Res 2006;46:658–664. [PubMed: 16039691]

van Hateren JH, Lamb TD. The photocurrent response of human cones is fast and monophasic. BMC Neurosci 2006;20:7–34.

Viswanathan S, Frishman LJ, Robson JG. Inner-retinal contributions to the photopic sinusoidal flicker electroretinogram of macaques. Doc Ophthalmol 2002;105:223–242. [PubMed: 12462445]

Wu J, Marmorstein AD, Kofuji P, Peachey NS. Contribution of Kir4.1 to the mouse electroretinogram. Mol Vis 2004;10:650–654. [PubMed: 15359216]

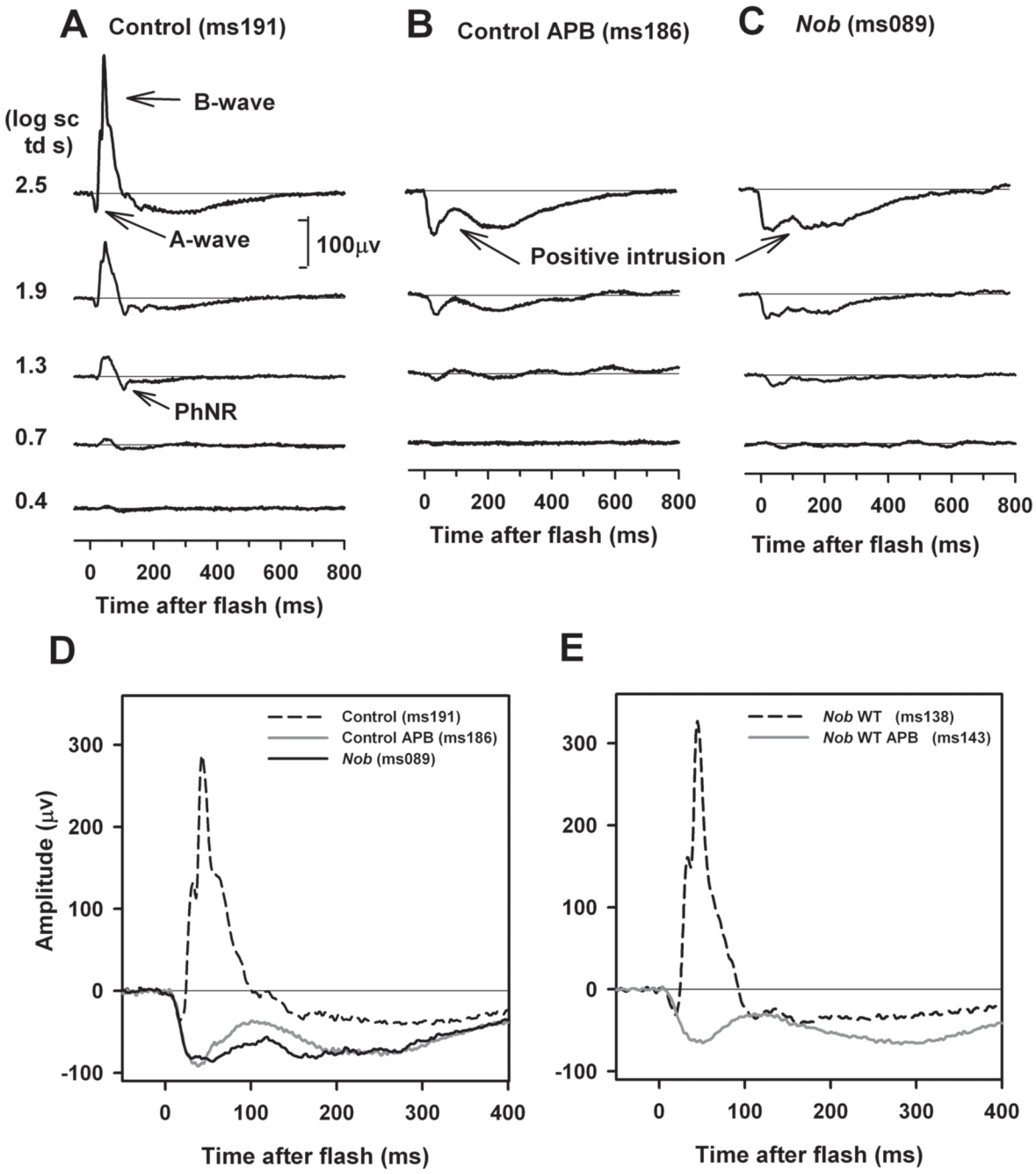

Figure 1. Light-adapted full field ERGs in response to brief flashes

Recordings are shown in response to brief LED flashes (λ max = 513 nm) of increasing stimulus energy on a rod saturating background (2.6 log sc td, λ max = 513 nm) for (A) a Control C57BL/6 mouse, (B) a Control C57BL/6 mouse after intravitreal injection of APB, and (C) a *Nob* mouse. (D) Superimposed ERGs of the Control mouse (dashed line), the Control mouse after APB injection (grey line) and *Nob* mouse (solid black line) in response to the highest energy stimulus in parts A–C. (E) Superimposed ERGs of a congenic wildtype control (*Nob* WT) mouse (dashed line) and *Nob* WT after APB injection (solid black line) in response to the highest energy stimulus. The mice in these experiments and in all figures prior to Fig. 6 were

three to six months of age. In this and all subsequent figures the number, MsXXX refers to the recording session for a given mouse.

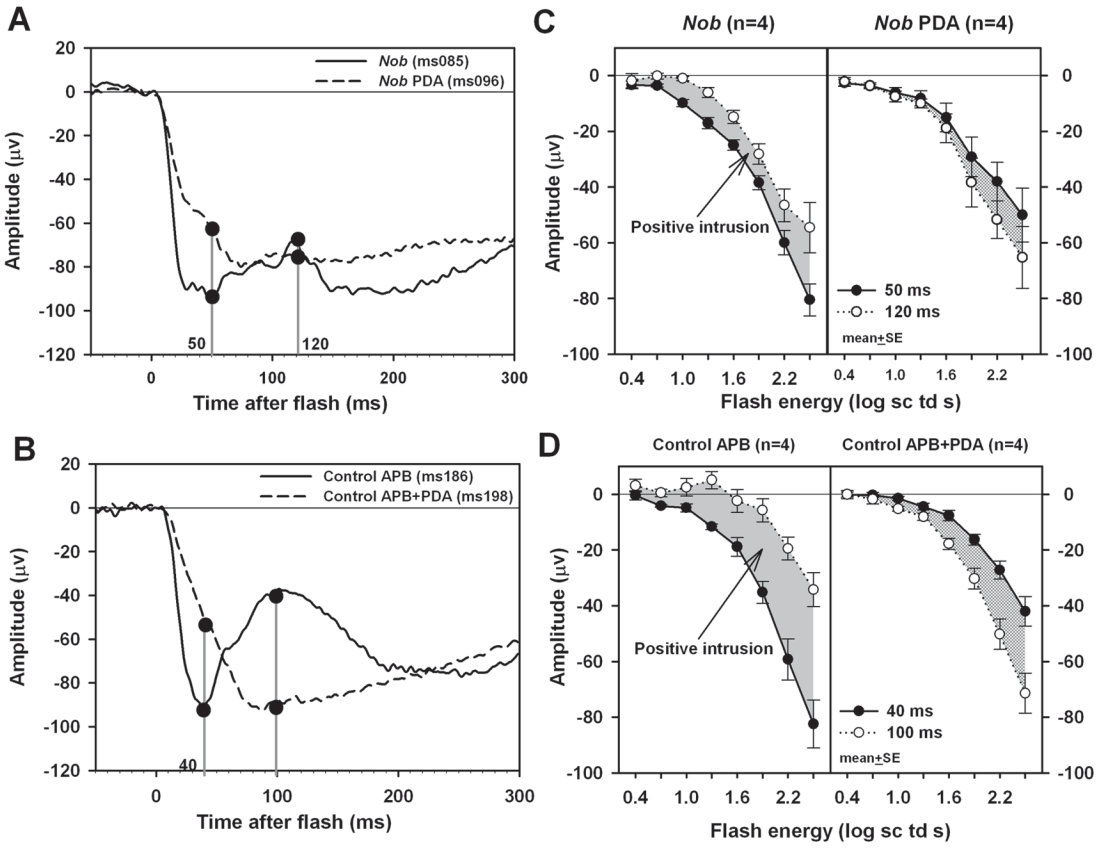

Figure 2. The positive intrusion in the brief-flash ERG of *Nob* and Control APB mice

(A) ERG of one *Nob* mouse before (solid line, recorded in an earlier session) and after (dashed line) injection of PDA, (B) ERG of one Control mouse with APB injected (solid line) in an earlier recording session, and after injection of APB+PDA (dashed line) in a later session. The vertical grey lines and filled black circles indicate the fixed times after the brief stimulus flash used to measure responses at the trough of the a-wave and the peak of the positive intrusion, (A) 50 ms and 120 ms for *Nob* mice, (B) 40 ms and 100 ms for Control APB mice. (C) Average response amplitudes for ERGs of *Nob* mice measured at 50 ms and 120 ms (left) after the stimulus flash, and (right) after PDA injection in the same eyes. The shaded areas represent the amplitude of the positive intrusion. (D) Average response amplitudes for four mice measured at 40 ms and 100 ms for (left) the Control mouse ERG after APB injection and (right) after APB+PDA injection. The shaded areas represent the amplitude of positive intrusion. The error bars = standard error of the mean (SE).

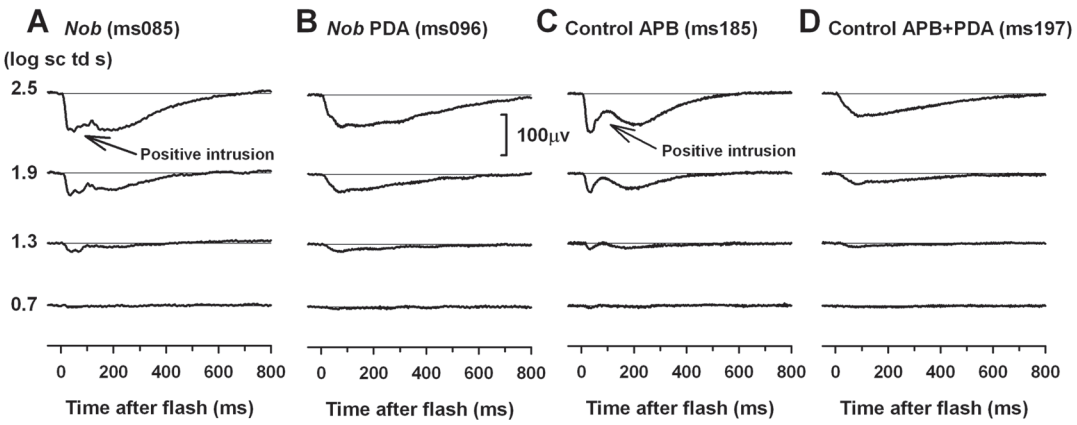

Figure 3. Effect of intravitreal PDA on the *Nob* and Control APB mouse ERG

Light-adapted full field ERGs obtained with brief flashes from (A) a *Nob* mouse (B) a *Nob* mouse after PDA injection, (C) a Control mouse after APB injection, (D) a Control mouse after APB+PDA injection.

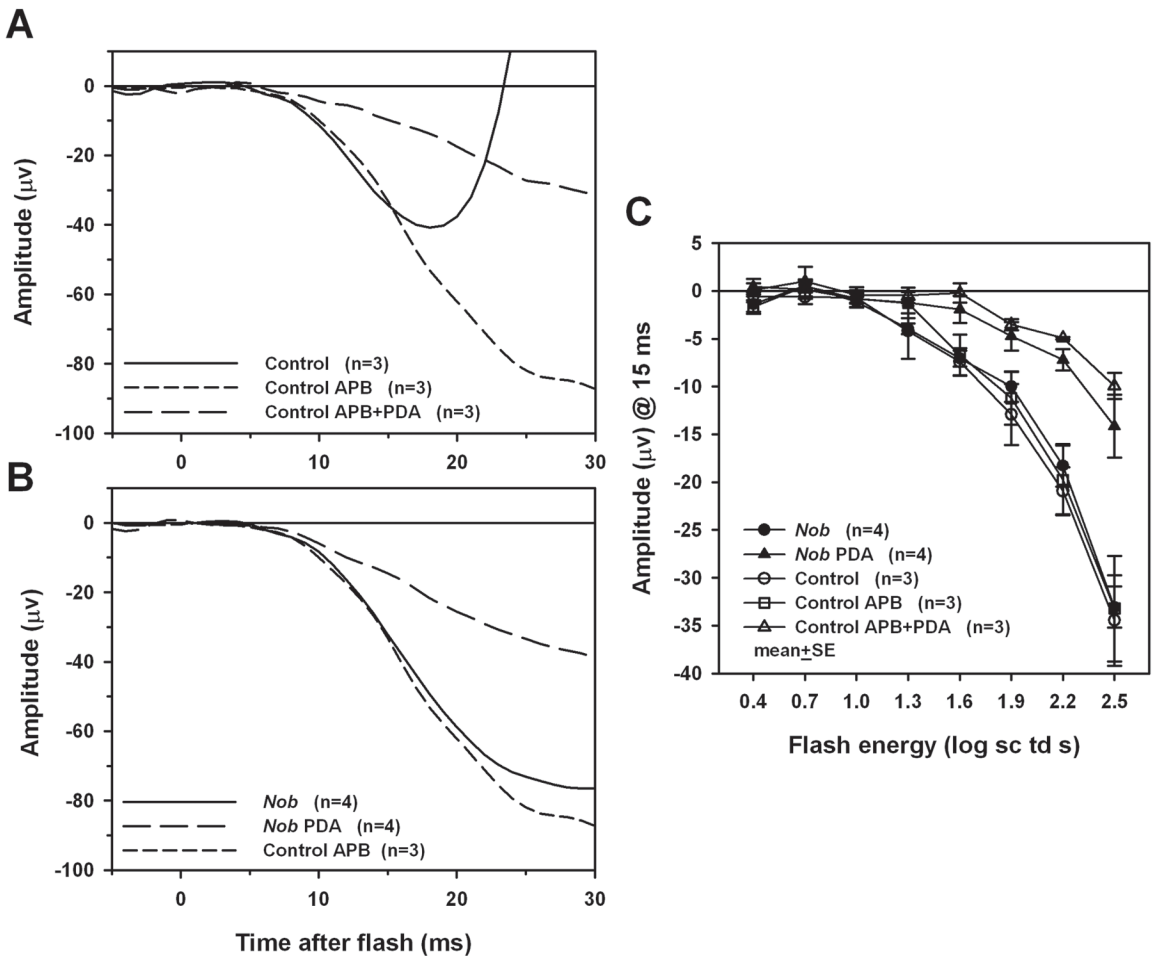

Figure 4. Effect of Intravitreal PDA on the a-wave in *Nob* and Control APB mice

(A) Plot of the leading edge of the light-adapted a-wave averaged for the Control mice (solid black line), Control mice after APB injection (short dashed line) and Control after APB+PDA injection (long dashed line), (B) Plot of the leading edge of the a-wave averaged for the Control mice after APB injection (short dashed line), *Nob* mice (sold black line), *Nob* mice after PDA injection (long dashed line). (C) Average ERG amplitudes for all experimental groups shown in parts A and B, measured at 15 ms after the flash, around the time of the a-wave trough in Control mice. The error bars = standard error of the mean (SE).

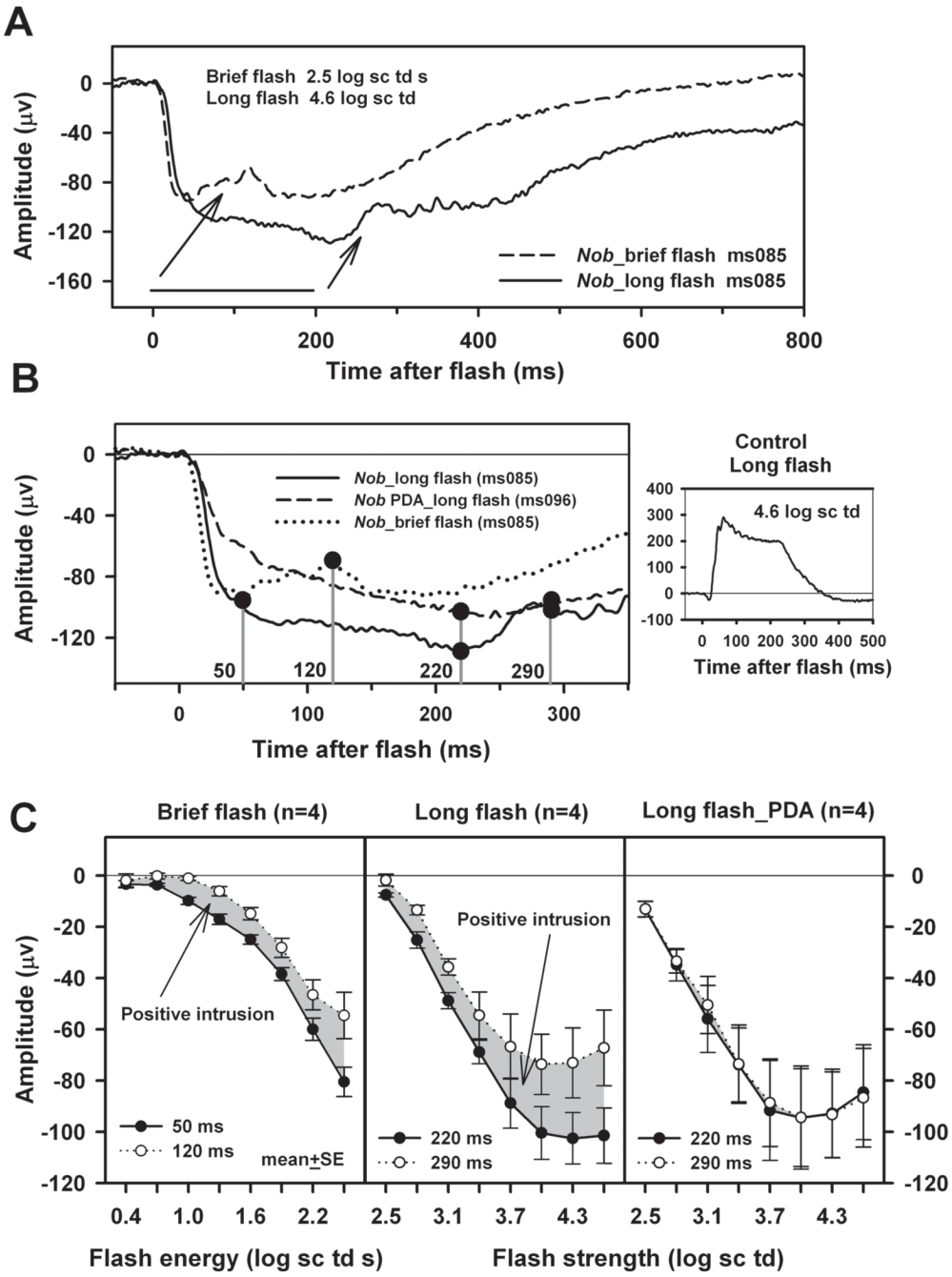

Figure 5. Light-adapted full field ERGs of *Nob* mice obtained using long duration flashes (200 ms)

(A) Response of one *Nob* mouse to a brief (dashed line) and a long flash (solid line); the arrows mark the positive intrusions in the two responses. (B) Responses from part A with the addition of the response to the long flash after PDA injection (dashed line). The grey vertical lines with filled circles indicate the fixed times after the brief flash for which response amplitudes were measured at the onset (50 ms) and peak (120 ms) of the positive intrusion; for the long flash, responses were measured after at light offset: 220 ms, and 290 ms from the onset of the 200 ms flash. Inset at right: response of a control mouse to the long flash of 4.6 log sc td. (C) Left: Average ERG response amplitudes measured at the times denoted in part B for four *Nob* mice in response to a brief flash. Middle: Average response amplitude of *Nob* mice to a long flash.

Right: Average response amplitude of *Nob* mice to a long flash after PDA injection. Shaded areas represent the positive intrusion amplitude of responses to: (left) brief flashes and (middle and right) long flashes. The error bars = standard error of the mean (SE).

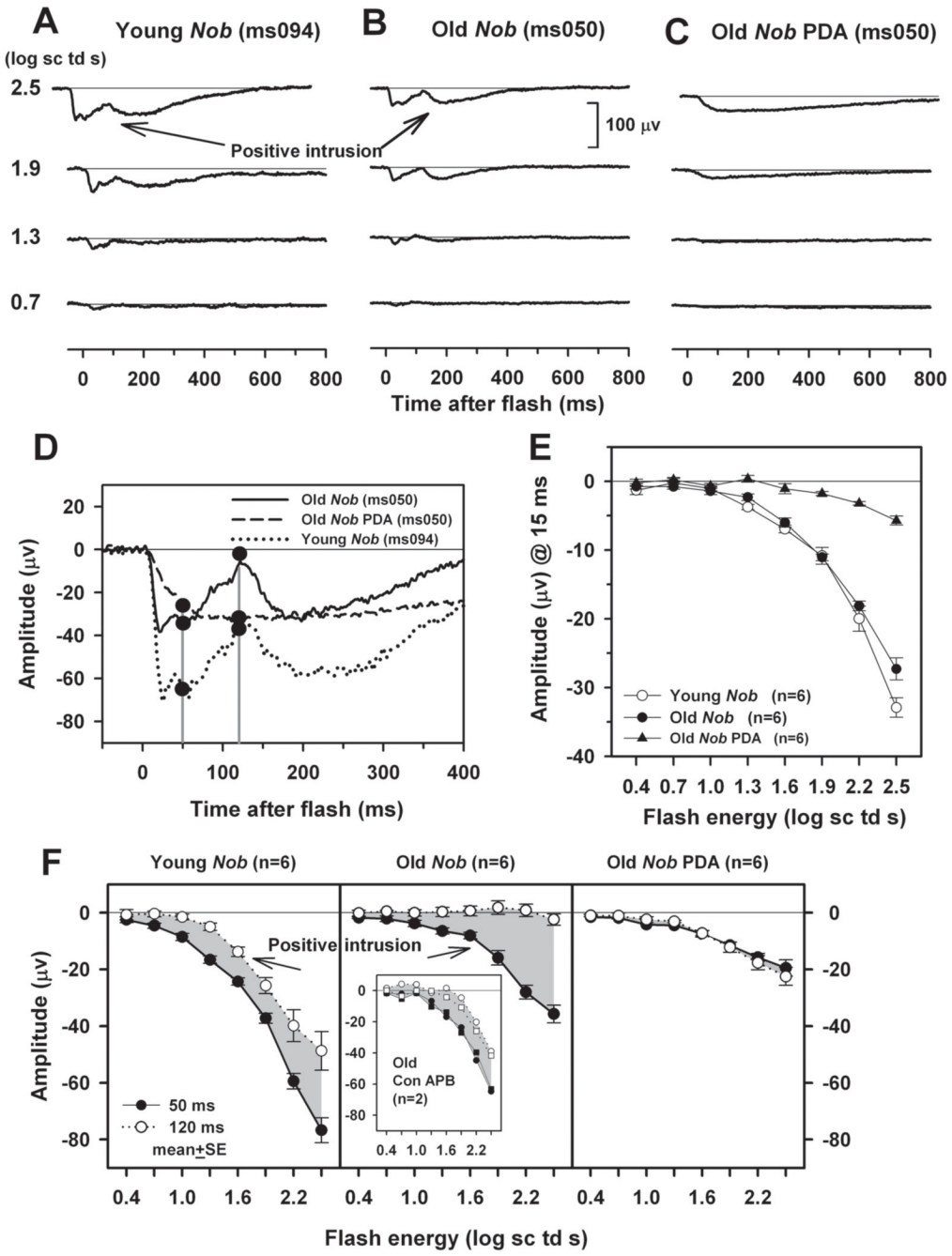

Figure 6. Comparison of the light-adapted ERGs of old and young *Nob* mice

(A) Light-adapted full field ERGs obtained with brief flashes for a young *Nob* mouse (three to six months old as in previous figures (B) ERGs from Old *Nob* mice, about one year of age, (C) Old *Nob* mice ERG after PDA injection. (D**)** Superimposed ERGs of Young *Nob*, Old *Nob* and Old *Nob* after PDA injection in response to the strongest stimuli, on expanded axes to visualize the positive intrusion. The vertical grey lines with black filled circle indicate the fixed measurement times for the onset and peak of the positive instruction: 50 ms and 120 ms. (E) Average a-wave amplitudes measured 15 ms after the flash for Young *Nob* mice (open circles), Old *Nob* mice (filled circles) and Old *Nob* mice after PDA injection (filled triangles). (F) Average ERG response amplitudes measured at 50 ms and 120 ms after the flash. Left:

Young *Nob* mice, Middle: Old *Nob*. Right: Old *Nob* after PDA injection. The shaded areas represent the amplitude of the positive intrusion. The error bars = standard error of the mean (SE).

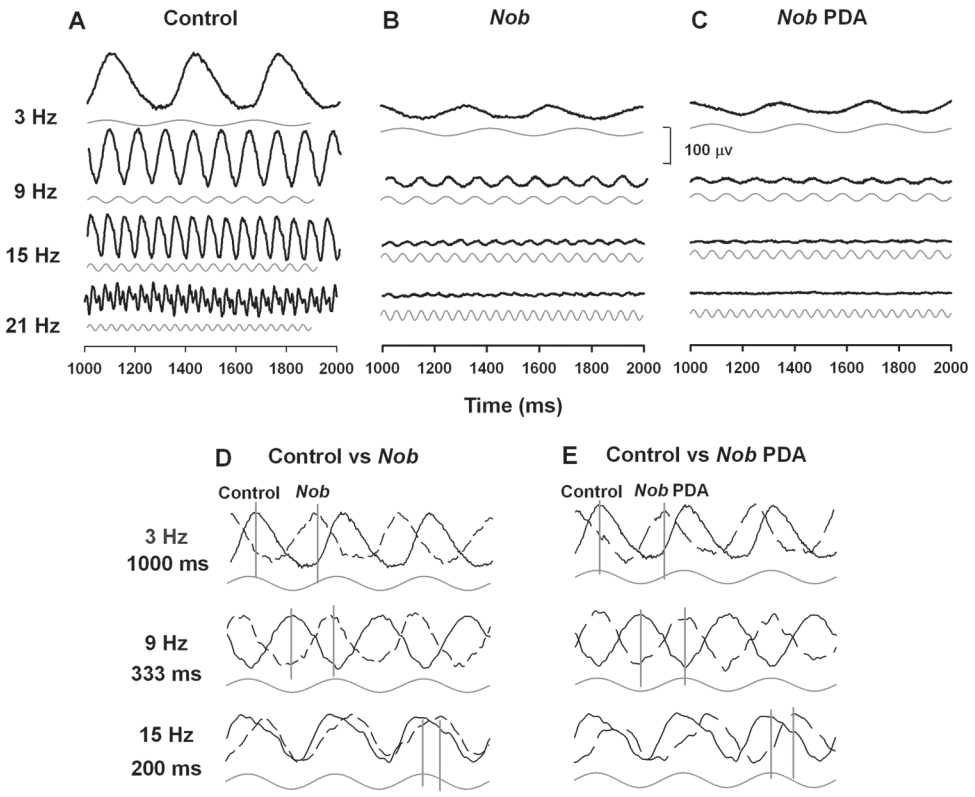

Figure 7. ERG responses of Control and *Nob* mice to sinusoidal stimulation (Flicker ERG)

Flicker ERGs in response to sinusoidal stimulation (indicated by grey lines) of a (A) Control mouse, (B) *Nob* mouse and (C) *Nob* mouse after PDA injection. Records were selected for analysis 1000 ms after the onset of the flicker, after the response had stabilized. (D) and (E) Superimposed ERGs of (D) Control and *Nob* mice, (E) Control and *Nob* mice after PDA injection. Grey vertical lines indicate peaks of cycles, first (left) for the Control mice and then for *Nob* mice. The stimuli for this figure and for Fig. 8–10 were sinusoidally modulated LEDs (mean luminance 2.6 log sc td; λ max = 513 nm; contrast 100 %).

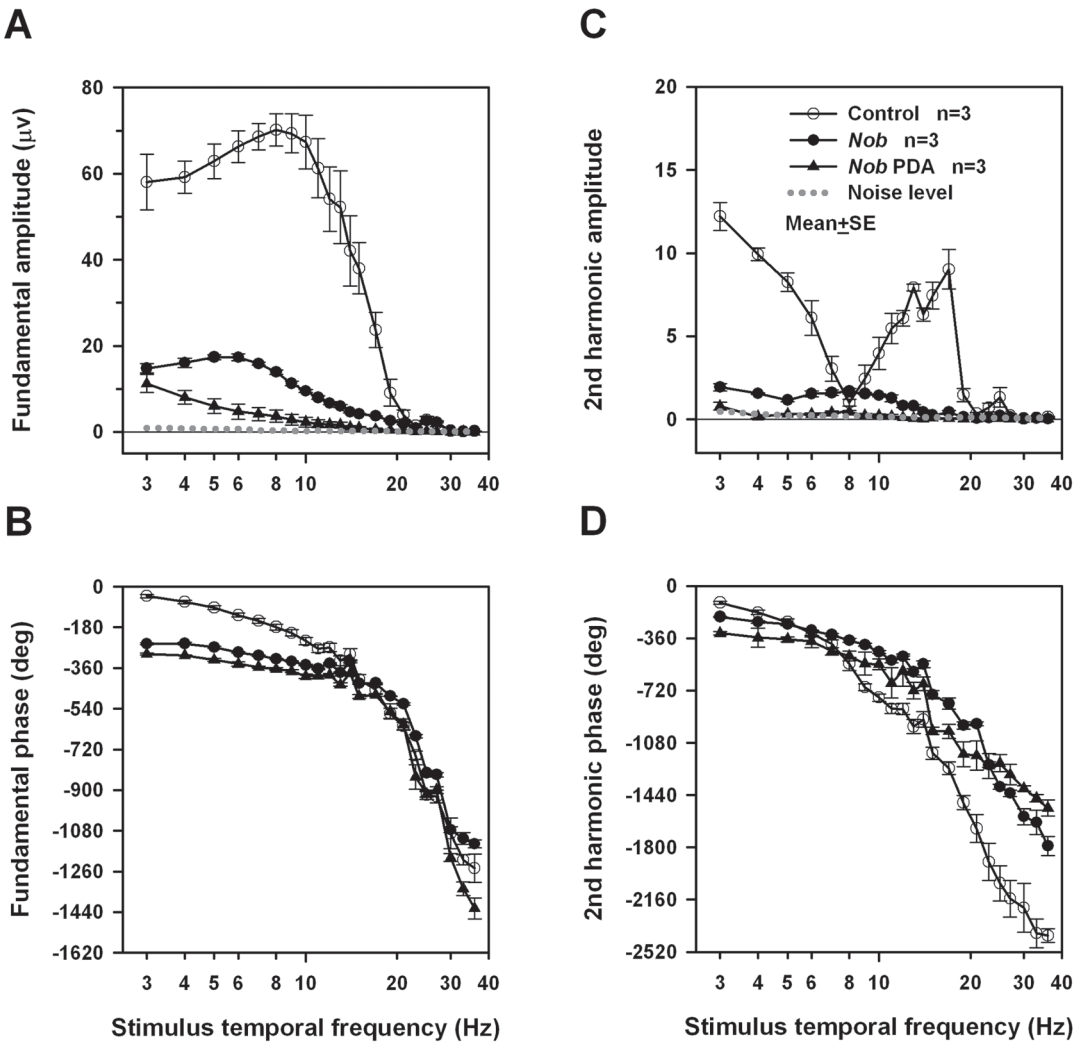

Figure 8. Temporal frequency response of Control and *Nob* mouse ERG

Plots of average amplitude (A, C) and phase (B, D) of the fundamental (A, B) and second harmonic (C, D) component of flicker ERGs. The open and filled black circles represent amplitudes of flicker ERGs of Control and *Nob* mice, and the filled triangles represent ERG responses of *Nob* mice after PDA injection. The error bars = standard error of the mean (SE). The filled grey circles in the amplitude plots (A and C) represent the average amplitude of the noise for each frequency, obtained from unmodulated (zero frequency) portions of the recordings.

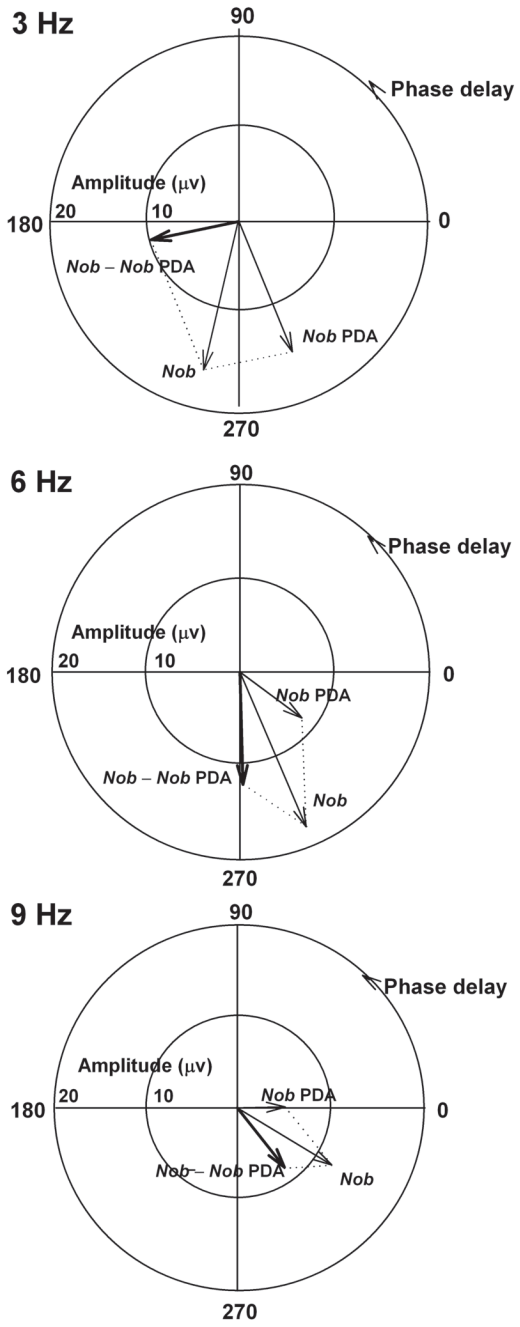

Figure 9. Vector analysis of the sinusoidal flicker ERG of *Nob* mice

The constituent amplitude and phase vectors for the fundamental frequency component of the 3 Hz, 6 Hz and 9 Hz flicker ERG of *Nob* mice. The thin arrows represent responses of *Nob* mice and *Nob* mice after PDA injection. Thick arrows represent PDA sensitive (postreceptoral) component derived as the difference between the *Nob* and the *Nob*+PDA response vectors.

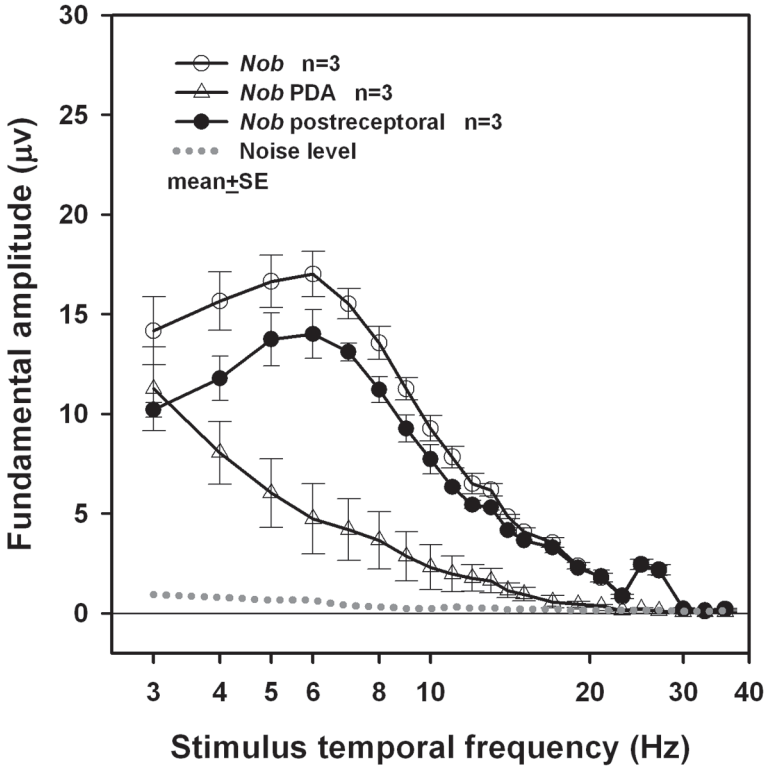

Figure 10. Postreceptoral component of the *Nob* mice sinusoidal flicker ERG

Plots of the average fundamental amplitude (F1) of the flicker ERG vs. temporal frequency for *Nob* mice (open circles), *Nob* mice after PDA injection (open triangles and the postreceptoral component of the *Nob* mouse ERG (filled circles) derived from vector analysis.

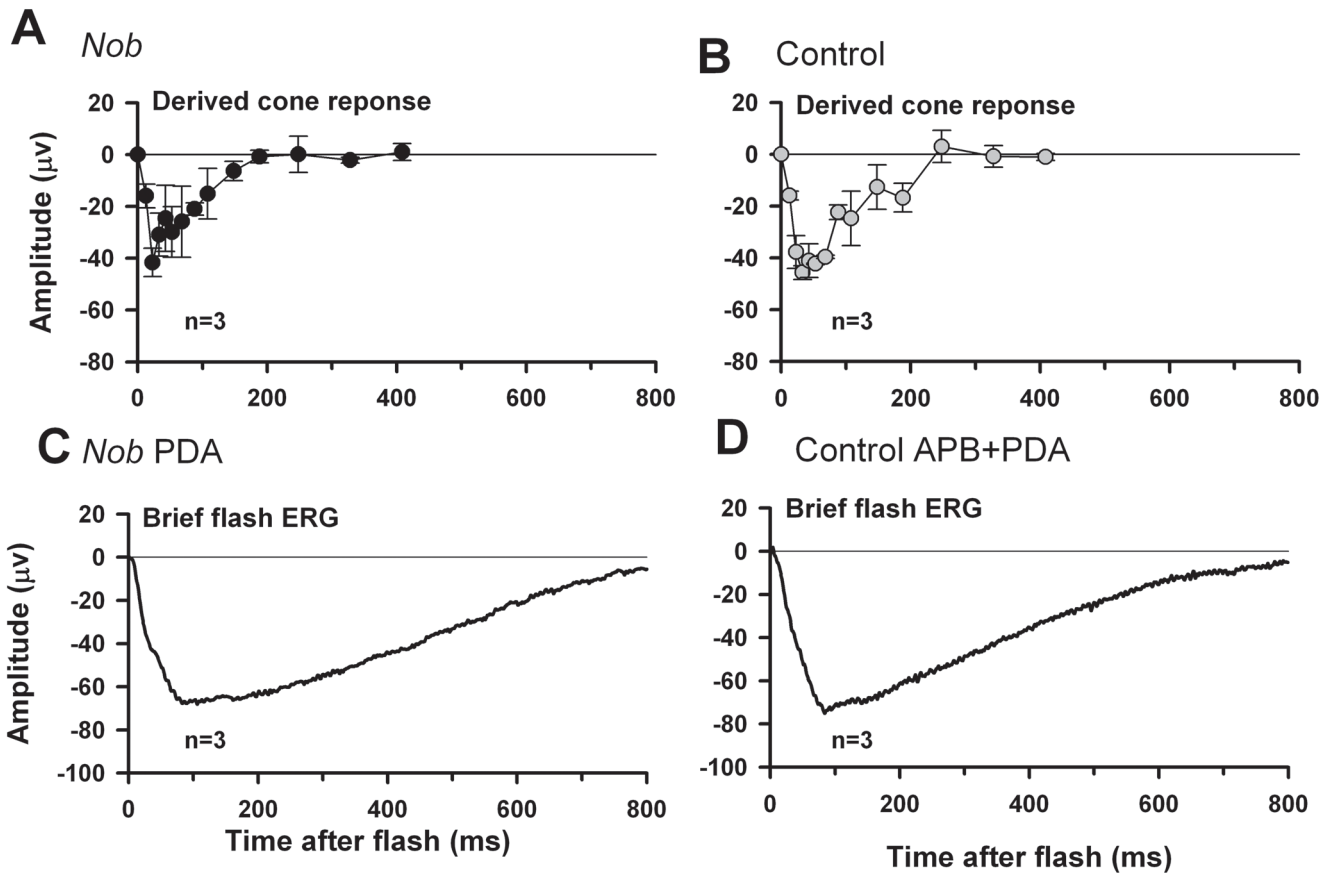

Figure 11. Derived cone photoreceptor response of the *Nob* and Control mouse

Average derived cone photoreceptor responses of (A) a *Nob* mouse and (B) a Control mouse (n=3 for both groups). Responses were derived for a flash strength of 2.5 log sc td s. (C and D) Average flash ERGs responses to the same flash strength are shown for three *Nob* mice after PDA injection and three Control mice after APB+PDA injection.